

# Tractable Evaluation of Stein's Unbiased Risk Estimator with Convex Regularizers

Parth Nobel\*      Emmanuel Candès<sup>†</sup>      Stephen Boyd\*

November 10, 2022

## Abstract

Stein's unbiased risk estimate (SURE) gives an unbiased estimate of the  $\ell_2$  risk of any estimator of the mean of a Gaussian random vector. We focus here on the case when the estimator minimizes a quadratic loss term plus a convex regularizer. For these estimators SURE can be evaluated analytically for a few special cases, and generically using recently developed general purpose methods for differentiating through convex optimization problems; these generic methods however do not scale to large problems. In this paper we describe methods for evaluating SURE that handle a wide class of estimators, and also scale to large problem sizes.

---

\*Department of Electrical Engineering, Stanford University

<sup>†</sup>Department of Statistics, Stanford University

# Contents

<b>1</b>	<b>Introduction and background</b>	<b>3</b>
1.1	Stein’s unbiased risk estimate (SURE)	3
1.2	Convex regularized regression	3
1.3	Classical examples	4
1.4	Matrix estimators	4
1.5	Algorithms for convex regularized regression	6
1.6	Weak differentiability of convex regularized regression	8
1.7	This paper	9
<b>2</b>	<b>SURE-CR</b>	<b>9</b>
2.1	Randomized trace estimation	9
2.2	Vector-Jacobian oracles	11
2.3	Implementation	14
<b>3</b>	<b>Numerical examples</b>	<b>14</b>
3.1	LASSO	16
3.2	Matrix completion	17
3.3	Robust PCA	20
3.4	SURE for hyperparameter selection	20
<b>A</b>	<b>Code examples</b>	<b>27</b>
A.1	CVXPYlayers — LASSO	27
A.2	LASSO	27
A.3	Matrix completion	28
A.4	Robust PCA	29
<b>B</b>	<b>Bound on the variance of SURE</b>	<b>30</b>
<b>C</b>	<b>Differentiating the proximal operator of the nuclear norm</b>	<b>31</b>
C.1	Gradient for full-rank and simple matrices	31
C.2	Extension by continuity to all matrices	32
C.3	Numerically stable computation	33

# 1 Introduction and background

## 1.1 Stein’s unbiased risk estimate (SURE)

We consider  $y \sim \mathcal{N}(\mu, \sigma^2 I)$  where  $\mu \in \mathbf{R}^d$  and  $I$  is the  $d \times d$  identity matrix. We assume  $\sigma$  is known and that we are estimating  $\mu$ . We are analyzing estimators  $\hat{\mu} : \mathbf{R}^d \rightarrow \mathbf{R}^d$  which estimate  $\mu$  given a single sample  $y$ . The  $\ell_2$  risk of an estimator  $\hat{\mu}$  is  $R(\hat{\mu}) = \mathbf{E} \|\hat{\mu}(y) - \mu\|_2^2$ .

In 1981, Charles Stein introduced in [33] what is now called Stein’s unbiased risk estimate,

$$\text{SURE}(\hat{\mu}, y) = -d\sigma^2 + \|\hat{\mu}(y) - y\|_2^2 + 2\sigma^2 \nabla \cdot \hat{\mu}(y), \quad (1)$$

where  $\nabla \cdot \hat{\mu}(y) = \sum_{i=1}^d \frac{\partial \hat{\mu}_i}{\partial y_i}(y)$  is the divergence of  $\hat{\mu}$  at  $y$ . The divergence can also be expressed as  $\nabla \cdot \hat{\mu}(y) = \mathbf{Tr}(D\hat{\mu}(y))$ , where  $D\hat{\mu}(y)$  is the  $d \times d$  Jacobian or derivative, evaluated at  $y$ , and  $\mathbf{Tr}$  denotes the trace of a matrix. Stein showed that the SURE statistic is an unbiased estimate of the risk in the sense that  $\mathbf{E} \text{SURE}(\hat{\mu}, y) = R(\hat{\mu})$ . The challenge in evaluating  $\text{SURE}(\hat{\mu}, y)$  is evaluating the divergence  $\nabla \cdot \hat{\mu}(y)$ .

In (1), it is assumed that the estimator  $\hat{\mu}$  is weakly differentiable and satisfies some integrability conditions. If this is not the case, SURE is not defined; we discuss this in more detail in §1.6.

## 1.2 Convex regularized regression

In this paper we consider the setting where  $\mu$  is a known linear function of unknown parameters  $\beta \in B$ , where  $\beta$  can be a vector, a matrix, or tuples of vectors and matrices, and  $B$  is the vector space of all such parameters, with dimension  $p$ . We will identify  $B$  with  $\mathbf{R}^p$ , using some fixed ordering of the entries of the vectors and matrices that comprise  $b \in B$ . For  $b \in B$ , we define  $\|b\|_2^2$  as the sum of the squares of the entries of  $b$ . In other words, we use  $\|b\|_2^2$  to mean the square of the  $\ell_2$  norm of  $b$ , interpreted as an element of  $\mathbf{R}^p$ . For example, if  $b$  is a matrix,  $\|b\|_2^2$  denotes its Frobenius norm, and not its induced  $\ell_2$  norm/maximum singular value. When  $b$  is a matrix and we wish to refer to its induced  $\ell_2$  norm, we use the notation  $\sigma_{\max}(b)$ .

We take  $\mu = \mathcal{A}\beta$ , where  $\mathcal{A} : B \rightarrow \mathbf{R}^d$  is linear. Using our identification of  $B$  and  $\mathbf{R}^p$ , we can represent  $\mathcal{A}$  explicitly as a  $d \times p$  matrix. But for purposes of computing, it is more convenient to keep it abstract. In the sequel we will denote the adjoint of the mapping as  $\mathcal{A}^*$ .

We consider estimators given by convex regularized regression, *i.e.*, of the form

$$\hat{\mu}(y) = \mathcal{A} \underset{b}{\operatorname{argmin}} \left( \frac{1}{2} \|\mathcal{A}b - y\|_2^2 + r(b) \right), \quad (2)$$

where  $r : B \rightarrow \mathbf{R} \cup \{\infty\}$  is a convex regularizer. The data in this problem are the linear mapping  $\mathcal{A}$ , the regularizer  $r$ , and the observed sample  $y$ . We will denote the argmin in (2) as  $\hat{\beta}(y)$  so that  $\hat{\mu}(y) = \mathcal{A}\hat{\beta}(y)$ . Many common estimators have this form. For some of these, there are closed form expressions for either  $\hat{\mu}(y)$  or SURE.

### 1.3 Classical examples

**Ordinary least squares.** In ordinary least squares,  $\mathcal{A}$  is a full-rank data matrix  $X \in \mathbf{R}^{d \times p}$  and

$$\hat{\mu}(y) = X \operatorname{argmin}_b \frac{1}{2} \|Xb - y\|_2^2 = X(X^*X)^{-1}X^*y.$$

With the orthogonal projection matrix  $H$  defined as  $H = X(X^*X)^{-1}X^*$ , we have

$$\text{SURE}(\hat{\mu}, y) = (2p - d)\sigma^2 + \|Hy - y\|_2^2.$$

**Ridge regression.** In ridge regression,  $\mathcal{A}$  is a potentially rank-deficient data matrix, and

$$\hat{\mu}(y) = X \operatorname{argmin}_b \left( \frac{1}{2} \|Xb - y\|_2^2 + \lambda \|b\|_2^2 \right) = X(X^*X + \lambda I)^{-1}X^*y,$$

where  $\lambda > 0$ . With  $H = X(X^*X + \lambda I)^{-1}X^*$ , we have

$$\text{SURE}(\hat{\mu}, y) = -d\sigma^2 + \|Hy - y\|_2^2 + 2\sigma^2 \operatorname{Tr} H.$$

**LASSO.** In LASSO,  $\mathcal{A}$  is again a data matrix, and

$$\hat{\mu}(y) = X \operatorname{argmin}_b \left( \frac{1}{2} \|Xb - y\|_2^2 + \lambda \|b\|_1 \right),$$

where  $\lambda > 0$ . There is no analytical formula for  $\hat{\mu}(y)$ , but it is readily evaluated numerically. In the usual case where the LASSO solution is unique, SURE takes the form

$$\text{SURE}(\hat{\mu}, y) = -d\sigma^2 + \|X\hat{\beta}(y) - y\|_2^2 + 2\sigma^2 \mathbf{card} \hat{\beta}(y),$$

where  $\mathbf{card}(\cdot)$  is the number of nonzero entries [36].

### 1.4 Matrix estimators

We now describe a few examples where  $\mathcal{A}$  is not a data matrix, and except for the first example, there are no known expressions for SURE.

**Singular value thresholding.** The first example is singular value thresholding, where  $y$  and  $\beta$  are matrices in  $B = \mathbf{R}^{m \times n}$  and

$$\hat{\mu}(y) = \underset{b}{\operatorname{argmin}} \left( \frac{1}{2} \|b - y\|_F^2 + \lambda \|b\|_* \right),$$

where  $\lambda > 0$  and  $\|\cdot\|_*$  is the nuclear norm, *i.e.*, the dual of the spectral norm, the sum of the singular values of  $b$ . Here we take  $\mathcal{A}$  to be the identity operator in our generic formulation. The estimator  $\hat{\mu}$  can be expressed analytically as singular value thresholding, *i.e.*,  $\hat{\mu}(y) = UF(\Sigma)V^*$ , where  $y = U\Sigma V^*$  is the singular value decomposition of  $y$ , and  $F(\Sigma)$  is the diagonal matrix with  $F(\Sigma)_{ii} = \max\{\Sigma_{ii} - \lambda, 0\}$ . A closed form expression for SURE in this case is given in [13].

**Matrix completion.** Our second example is matrix completion, which extends singular value thresholding to the setting where only some entries of a matrix are observed. As in singular value thresholding, we have  $\beta \in B = \mathbf{R}^{m \times n}$ . In matrix completion,  $\mathcal{A} : B \rightarrow \mathbf{R}^d$  is a selection operator, with  $d$  the number of entries of  $\beta$  that are being observed (hence, the observation  $\mu$  is a vector containing the observed entries of the matrix). A selection operator takes certain entries of  $\beta$  and returns their value while ignoring all other entries. The estimator is

$$\hat{\mu}(y) = \mathcal{A} \underset{b}{\operatorname{argmin}} \left( \frac{1}{2} \|\mathcal{A}b - y\|_2^2 + \lambda \|b\|_* \right),$$

where  $\lambda > 0$ . Unlike singular value thresholding, there is no known analytical expression for  $\hat{\mu}(y)$ , but it is readily evaluated. Also, there is no known closed-form expression for SURE for matrix completion which can be tractably evaluated.

For future use we note that  $\hat{\beta}(y) = 0$  if and only if

$$\lambda \geq \lambda_{\max} = \sigma_{\max}(\mathcal{A}^*y), \quad (3)$$

where  $\mathcal{A}^*y$  is a matrix which satisfies  $\mathcal{A}\mathcal{A}^*y = y$  and which has all entries not uniquely determined by that equation equal to 0.

**Robust PCA.** Our final example is robust PCA, where

$$b = (L, S) \in \mathbf{R}^{m \times n} \times \mathbf{R}^{m \times n}$$

and  $\mathcal{A}(L, S) = L + S$ . For completeness, we note that  $\mathcal{A}^*V = (V, V)$  where  $V$  is any matrix. The estimator is given by

$$\hat{\mu}(y) = \underset{L, S}{\operatorname{argmin}} \left( \frac{1}{2} \|\mathcal{A}(L, S) - y\|_F^2 + \lambda \|L\|_* + \gamma \|S\|_1 \right),$$

where  $\lambda > 0$  and  $\gamma > 0$ . There is no known closed-form expression for  $\hat{\mu}(y)$ , but it is readily evaluated. There is no known closed-form expression for SURE.

Here too we can determine the values of  $\lambda$  and  $\gamma$  for which the optimal solution obeys  $\hat{\beta}(y) = 0$ . We have  $\hat{\beta}(y) = 0$  if and only if

$$\lambda \geq \lambda_{\max} = \sigma_{\max}(y) \quad \text{and} \quad \gamma \geq \gamma_{\max} = \|y\|_{\infty}, \quad (4)$$

where  $\|y\|_{\infty} = \max_{i,j} |y_{ij}|$ . We are not aware of this result appearing in the literature, so we give a short derivation here. The necessary and sufficient optimality condition for  $L$  and  $S$  is

$$L + S - y + \lambda \partial \|L\|_* \ni 0, \quad L + S - y + \gamma \partial \|S\|_1 \ni 0,$$

where  $\partial$  denotes the subdifferential. Applying this to  $L = S = 0$  we have that  $L = S = 0$  is optimal if and only if

$$y \in \lambda \partial \|0\|_*, \quad y \in \gamma \partial \|0\|_1.$$

Using the fact that the subdifferential of a norm at zero is the unit ball of the dual norm, we can write this as (4).

## 1.5 Algorithms for convex regularized regression

Several algorithms for evaluating the estimator (2) access the data  $\mathcal{A}$  and  $r$  in the following restricted way: the linear operator  $\mathcal{A}$  is accessed only through its forward and adjoint oracle. This means we can evaluate  $\mathcal{A}b$  for any  $b \in B$ , and  $\mathcal{A}^*z$  for any  $z \in \mathbf{R}^d$ , where  $\mathcal{A}^* : \mathbf{R}^d \rightarrow B$  is the adjoint of  $\mathcal{A}$ . This allows us to handle problems without forming or storing an explicit matrix representation of  $\mathcal{A}$ .

The regularizer is accessed only via its proximal operator  $\mathbf{prox}_{tr} : B \rightarrow B$ , given by

$$\mathbf{prox}_{tr}(v) = \underset{b}{\operatorname{argmin}} \left( tr(b) + \frac{1}{2} \|b - v\|_2^2 \right),$$

where  $v, b \in B$  and  $t$  is a positive scalar that can be interpreted (in the context of algorithms) as a step length. Thus our access to the regularizer is via its proximal operator, *i.e.*, we can evaluate  $\mathbf{prox}_{tr}(v)$  for any  $v$ . The proximal operators of many common regularizers are known and readily computed [7, 15, 26, 29].

As examples, in LASSO,  $r(b) = \lambda \|b\|_1$ , and its proximal operator is given elementwise by

$$(\mathbf{prox}_{tr}(v))_i = \begin{cases} v_i - t\lambda & \text{if } v_i > t\lambda \\ -v_i + t\lambda & \text{if } v_i < -t\lambda \\ 0 & \text{else} \end{cases}.$$

This function is known as soft-thresholding and we denote it  $\mathcal{T}_{t\lambda}$ .

In matrix completion,  $r(b) = \lambda\|b\|_*$  and  $\mathbf{prox}_{tr}(v)$  is given by singular value thresholding with regularization parameter  $t\lambda$ . In robust PCA,  $r((L, S)) = \lambda\|L\|_* + \gamma\|S\|_1$  is separable with respect to  $L$  and  $S$ . Therefore,

$$\begin{aligned}\mathbf{prox}_{tr}((L, S)) &= \operatorname{argmin}_{L', S'} \left( t(\lambda\|L'\|_* + \gamma\|S'\|_1) + \frac{1}{2}\|(L', S') - (L, S)\|_2^2 \right) \\ &= \operatorname{argmin}_{L', S'} \left( t\lambda\|L'\|_* + t\gamma\|S'\|_1 + \frac{1}{2}\|(L' - L, S' - S)\|_2^2 \right) \\ &= \operatorname{argmin}_{L', S'} \left( t\lambda\|L'\|_* + t\gamma\|S'\|_1 + \frac{1}{2}\|L' - L\|_2^2 + \frac{1}{2}\|S' - S\|_2^2 \right) \\ &= \left( \operatorname{argmin}_{L'} \left( t\lambda\|L'\|_* + \frac{1}{2}\|L' - L\|_2^2 \right), \operatorname{argmin}_{S'} \left( t\gamma\|S'\|_1 + \frac{1}{2}\|S' - S\|_2^2 \right) \right) \\ &= \left( \mathbf{prox}_{t\lambda\|\cdot\|_*}(L), \mathbf{prox}_{t\gamma\|\cdot\|_1}(S) \right).\end{aligned}$$

These two proximal operators are exactly those in LASSO and matrix completion.

We now mention three algorithms that only require oracle access to  $\mathcal{A}$ ,  $\mathcal{A}^*$ , and  $\mathbf{prox}_{tr}(\cdot)$ .

**ISTA.** The proximal gradient method (also known as ISTA) [7, 8, 29] consists of the iterations

$$b^{k+1} = \mathbf{prox}_{tr} \left( b^k - t\mathcal{A}^* (\mathcal{A}b^k - y) \right).$$

The algorithm itself requires only multiplication by  $\mathcal{A}$  and  $\mathcal{A}^*$ . The step length  $t$  must satisfy  $t \leq 2/\sigma_{\max}(\mathcal{A})$  to guarantee convergence [29, §4.2]; here,  $\sigma_{\max}(\mathcal{A})$  is the induced  $\ell_2$  norm, which can be computed by a power algorithm that only uses multiplication by  $\mathcal{A}$  and  $\mathcal{A}^*$ . For our purposes, ISTA can be initialized with any vector which is selected independently of  $y$ .

**FISTA.** The accelerated proximal gradient method (also known as FISTA) [7, 8, 29] consists of adding a momentum term to the proximal gradient method to obtain the iterations

$$\begin{aligned}\tau^{k+1} &= \frac{1 + \sqrt{1 + 4(\tau^k)^2}}{2} \\ b^{k+1/2} &= b^k + \frac{\tau^k - 1}{\tau^{k+1}} (b^k - b^{k-1}) \\ b^{k+1} &= \mathbf{prox}_{tr} \left( b^{k+1/2} - t\mathcal{A}^* (\mathcal{A}b^{k+1/2} - y) \right),\end{aligned}$$

where  $k$  is the iteration counter and  $\tau_1 = 1$ . The algorithm itself requires only multiplication by  $\mathcal{A}$  and  $\mathcal{A}^*$ . The step length  $t$  must satisfy  $t \leq 1/\sigma_{\max}(\mathcal{A})$  to guarantee convergence [29, §4.3]. It is also possible to use  $\tau^k = \frac{k+2}{2}$  [7, Remark 10.35], as we do in the sequel. For our purposes, FISTA can be initialized with any vector  $b^1$  which is selected independent of  $y$ . FISTA is almost always preferable to ISTA.

**ADMM.** The third algorithm we mention is the alternating direction method of multipliers (ADMM) [12], with iterations

$$\begin{aligned} b^{k+1} &= \mathbf{prox}_{tr}(z^k - u^k) \\ z^{k+1} &= (t\mathcal{A}^*\mathcal{A} + I)^{-1}(b^{k+1} + u^k + t\mathcal{A}^*y) \\ u^{k+1} &= u^k + b^{k+1} - z^{k+1}, \end{aligned}$$

where  $u^k, z^k \in B$ . For ADMM, the parameter  $t$  can take any positive value. To compute the update step for  $z^{k+1}$  we need to solve a positive-definite system of equations by only accessing  $\mathcal{A}^*$  and  $\mathcal{A}$ . There are many methods to do this, for example, conjugate-gradient (CG) type methods [22, 24, 31].

For all of these algorithms,  $b^k$  converges to a solution of (2). There are many other algorithms for evaluating these estimators; see, *e.g.*, [7, 14, 27, 28, 32]. The methods for computing SURE we describe below will work with most of these as well.

## 1.6 Weak differentiability of convex regularized regression

For SURE to be an unbiased estimate of risk, the estimator  $\hat{\mu}$  must be weakly differentiable and obey some integrability conditions. For our purpose, it is sufficient to show that  $\hat{\mu}$  is Lipschitz continuous [13, Lemma III.2].

We will now show that  $\hat{\mu}$  is Lipschitz if  $r$  is a closed convex proper function. The coefficient estimate  $\hat{\beta}(y)$  minimizes  $r(b) + \frac{1}{2}\|\mathcal{A}b - y\|_2^2$ , and so satisfies the optimality conditions

$$\partial r(\hat{\beta}(y)) + \mathcal{A}^*(\mathcal{A}\hat{\beta}(y) - y) \ni 0,$$

which implies that

$$\mathcal{A}^*y - \mathcal{A}^*\mathcal{A}\hat{\beta}(y) \in \partial r(\hat{\beta}(y)).$$

Evaluating  $\hat{\beta}$  at a second point  $\tilde{y}$  we find

$$\mathcal{A}^*\tilde{y} - \mathcal{A}^*\mathcal{A}\hat{\beta}(\tilde{y}) \in \partial r(\hat{\beta}(\tilde{y})).$$

By the subgradient inequality, we have for all  $w$

$$r(w) \geq r(\hat{\beta}(y)) + \langle \mathcal{A}^*y - \mathcal{A}^*\mathcal{A}\hat{\beta}(y) \mid w - \hat{\beta}(y) \rangle.$$

Evaluating this at  $w = \hat{\beta}(\tilde{y})$  gives

$$r(\hat{\beta}(\tilde{y})) \geq r(\hat{\beta}(y)) + \langle \mathcal{A}^*y - \mathcal{A}^*\mathcal{A}\hat{\beta}(y) \mid \hat{\beta}(\tilde{y}) - \hat{\beta}(y) \rangle,$$

and switching the roles of  $y$  and  $\tilde{y}$ , we obtain

$$r(\hat{\beta}(y)) \geq r(\hat{\beta}(\tilde{y})) + \langle \mathcal{A}^* \tilde{y} - \mathcal{A}^* \mathcal{A} \hat{\beta}(\tilde{y}) \mid \hat{\beta}(y) - \hat{\beta}(\tilde{y}) \rangle.$$

Adding these two inequalities yields

$$\begin{aligned} 0 &\geq \langle \mathcal{A}^* y - \mathcal{A}^* \mathcal{A} \hat{\beta}(y) \mid \hat{\beta}(\tilde{y}) - \hat{\beta}(y) \rangle + \langle \mathcal{A}^* \tilde{y} - \mathcal{A}^* \mathcal{A} \hat{\beta}(\tilde{y}) \mid \hat{\beta}(y) - \hat{\beta}(\tilde{y}) \rangle \\ &= \langle y - \mathcal{A} \hat{\beta}(y) \mid \mathcal{A} \hat{\beta}(\tilde{y}) - \mathcal{A} \hat{\beta}(y) \rangle + \langle \tilde{y} - \mathcal{A} \hat{\beta}(\tilde{y}) \mid \mathcal{A} \hat{\beta}(y) - \mathcal{A} \hat{\beta}(\tilde{y}) \rangle \\ &= \langle y - \hat{\mu}(y) - \tilde{y} + \hat{\mu}(\tilde{y}) \mid \hat{\mu}(\tilde{y}) - \hat{\mu}(y) \rangle \\ &= \langle y - \tilde{y} \mid \hat{\mu}(\tilde{y}) - \hat{\mu}(y) \rangle + \|\hat{\mu}(\tilde{y}) - \hat{\mu}(y)\|_2^2, \end{aligned}$$

using  $\mathcal{A} \hat{\beta}(y) = \hat{\mu}(y)$  and  $\mathcal{A} \hat{\beta}(\tilde{y}) = \hat{\mu}(\tilde{y})$  in the third line. Re-arranging and using the Cauchy-Schwartz inequality gives

$$\|\hat{\mu}(\tilde{y}) - \hat{\mu}(y)\|_2^2 \leq \langle \tilde{y} - y \mid \hat{\mu}(\tilde{y}) - \hat{\mu}(y) \rangle \leq \|\tilde{y} - y\|_2 \|\hat{\mu}(\tilde{y}) - \hat{\mu}(y)\|_2,$$

and so

$$\|\hat{\mu}(\tilde{y}) - \hat{\mu}(y)\|_2 \leq \|\tilde{y} - y\|_2,$$

which shows that  $\hat{\mu}$  is 1-Lipschitz.

## 1.7 This paper

In this paper we introduce an algorithm to tractably compute SURE for convex regularized regression, relying solely on a proximal operator oracle for the regularizer and a forward-adjoint oracle for  $\mathcal{A}$  and  $\mathcal{A}^*$ . Our algorithm, which we call SURE-CR, easily scales to problems with numbers of parameters  $b$  in the millions, where forming or storing the matrix  $D\hat{\mu}(y)$  would be impossible.

## 2 SURE-CR

### 2.1 Randomized trace estimation

In this section we describe methods for estimating the trace of a  $d \times d$  matrix  $M$ , that access  $M$  only via an oracle that evaluates its adjoint,  $v \mapsto M^*v$ . We refer to this oracle as vector-matrix oracle, since it evaluates (the transpose of)  $v^*M$ . We will apply this to the specific matrix  $M = D\hat{\mu}(y)$  to evaluate the divergence term in SURE.

The naïve approach is to use the oracle to evaluate  $M^*e_i$ , where  $e_i$  is the  $i$ th unit vector, for  $i = 1, \dots, d$ , whereupon we can readily evaluate

$$\mathbf{Tr} M = \sum_{i=1}^d e_i^*(M^*e_i).$$

When  $d$  is very large, this is slow. It also evidently involves much wasted computation, since we end up computing all  $d^2$  entries of  $M$ , only to sum the  $d$  diagonal ones.

Randomized methods can be used to estimate  $\mathbf{Tr} M$  using far fewer than  $d$  evaluations of the adjoint mapping. These methods are based on the simple observation that if the random variable  $Z \in \mathbf{R}^d$  satisfies  $\mathbf{E} Z = 0$  and  $\mathbf{E} Z Z^* = I$ , then we have  $\mathbf{E} Z^* M Z = \mathbf{Tr} M$ . To approximate this we compute  $m$  independent samples of  $Z$ ,  $z_1, \dots, z_m$ , and take the empirical mean as our estimate,

$$\mathbf{Tr} M \approx \frac{1}{m} \sum_{i=1}^m z_i^*(M^*z_i),$$

which is unbiased. In [23], Hutchinson showed that the variance of the error in this approximation is minimized if the  $Z_i$ 's are i.i.d. random variables taking pn values  $\pm 1$ , each with probability  $1/2$ .

Improvements on this basic randomized method were recently suggested by Meyer, Musco, Musco, and Woodruff in [25]. They proposed Hutch++, which uses a low-rank approximation of the matrix to project some queries away from large singular values of the matrix. Hutch++ is also an unbiased estimator of the trace, and consistently produces a good estimate of the trace using fewer queries to the vector-matrix oracle than the basic randomized method. Hutch++'s computation takes part in three phases, each of which require an equal number of calls to the vector-matrix oracle, so the total number of queries is a multiple of 3. In the first phase, Hutch++ sketches the matrix. In the second phase, it computes the exact trace of  $M$  projected onto the dominant dimensions found via the sketch. In the third phase, it runs the Hutchinson estimator on  $M$  projected away from those dominant dimensions.

In our method for evaluating SURE, we found that 34 queries per phase, for a total of 102 vector-matrix oracle calls, consistently produced high quality estimates of the trace. For small problems, *i.e.*, those of size less than or equal to 102, we exactly compute the trace without any randomization.

## 2.2 Vector-Jacobian oracles

In this section we describe methods for computing the adjoint oracle  $v \mapsto (D\hat{\mu}(y))^* v$ . Using  $\hat{\mu}(y) = \mathcal{A}\hat{\beta}(y)$ , we have  $D\hat{\mu}(y) = \mathcal{A}D\hat{\beta}(y)$  and, therefore,

$$(D\hat{\mu}(y))^* v = \left(D\hat{\beta}(y)\right)^* (\mathcal{A}^* v).$$

So it suffices to evaluate the mapping  $u \mapsto \left(D\hat{\beta}(y)\right)^* u$ . Roughly speaking, we need to differentiate through the solution of the optimization problem (2), *i.e.*, the mapping from the data  $y$  to the parameter estimate  $\hat{\beta}(y)$ .

**Differentiability.** In many cases  $\hat{\mu}$  is not differentiable. However in §1.6 we showed that  $\hat{\mu}$  is Lipschitz; by applying Rademacher’s theorem, we know that  $\hat{\mu}$  is a.e.-differentiable under the Lebesgue measure, and since  $y$  has a Gaussian distribution  $\hat{\mu}$  is almost surely differentiable at  $y$  [17, §3.1.2].

**Generic methods.** Some recent work shows how to differentiate through the solution of some convex optimization problems (when the mapping is differentiable), for example [5] for quadratic programs (QPs) and [3] for cone programs. These methods in turn have been integrated into software frameworks for automatic differentiation such as PyTorch [30] and TensorFlow [1, 4]. Such libraries include CVXPYlayers, diffcp, and OPTNET [2, 3, 5]. All of these give methods for evaluating  $u \mapsto D\hat{\beta}(y)^* u$ , without forming the matrix  $D\hat{\beta}(y)$ . These generic methods work well for small problems and some medium-sized problems, but they do not scale to large scale problems. At non-differentiable points, these methods compute a heuristic quantity [21, §14].

**Differentiating through an iterative solver.** Another approach to differentiating through a convex problem relies on a solver or iterative solution algorithm, such as those described in §1.5. Existing work differentiates through proximal operators to use them as non-linear activations in neural networks [16, 34], in this work, we differentiate through iterative optimization algorithms to approximate differentiating the solution map. Here we view the iterative algorithm as a sequence of mappings, *i.e.*, we view our iterative algorithm as applying an operator  $F^k$  at each iteration such that

$$b^{k+1}, S^{k+1} = F^k(b^k, S^k, y)$$

where  $S^k$  is any ancillary state in the algorithm (*e.g.*, in FISTA  $S^k = b^{k-1}$  and in ADMM  $S^k = (z^k, u^k)$ ). Suppose it takes  $\ell$  iterations to converge to a reasonable

tolerance, so  $\hat{\mu}(y) \approx F^\ell(F^{\ell-1}(\dots, y), y)$ . By implicitly differentiating this recurrence and applying the chain rule, we obtain a series of equations that we use to compute  $(D\hat{\mu}(y))^*v$ , given a vector of output sensitivities  $v$ . Our approximation of  $\hat{\mu}$  may be non-differentiable on a set of positive Lebesgue measure. In this situation, we need to compute a quantity that can serve as a surrogate for the true vector-Jacobian product. In neural network training, it is common to discuss the vector-Jacobian of a scalar loss function—which is simply the gradient—even when the loss function is non-differentiable. Many choices of surrogates when differentiability fails have been proposed and seem to work well here [11, 19]. In §3.2, our empirical results show that a continuous extension of the true derivative yields sufficiently accurate estimates at non-differentiable points of the derivative of  $\hat{\mu}$  so that we still have a good estimate of the risk of  $\hat{\mu}$ .

As an example of differentiating our approximation of  $\hat{\mu}$ , we work through the derivative of ISTA. ISTA is straightforward to analyze because there is no ancillary state in the algorithm, but this methods easily generalize to the other algorithms from §1.5. To simplify our equations, we let  $b^{k+1/2} = b^k - t\mathcal{A}^*(\mathcal{A}b^k - y)$ . By differentiating the ISTA iterations we obtain

$$\begin{aligned} Db^{k+1} &= D\text{prox}_{tr}(b^{k+1/2}) Db^k - t\mathcal{A}^*(\mathcal{A}Db^k - I) \\ &= (D\text{prox}_{tr}(b^{k+1/2}) - t\mathcal{A}^*\mathcal{A}) Db^k + t\mathcal{A}^*. \end{aligned}$$

In a forward pass, we can evaluate  $b^{k+1/2}$  for  $k = 1, \dots, \ell - 1$  and cache them to enable the vector-Jacobian oracle evaluations. Evaluating  $(Db^\ell)^*v$  then becomes a recursive problem, which can be computed using two of the oracles we needed for the forward pass— $\mathcal{A}$  and  $\mathcal{A}^*$ —and one new oracle: the vector-Jacobian oracle for the proximal operator. The base case for our recursion comes from our requirement that  $b^1$  is chosen independently of  $y$  *i.e.* that  $(Db^1)^*v = 0$ . The difficulty in this method relies in evaluating the vector-Jacobian oracle of the proximal operator.

**Evaluating proximal operator vector-Jacobian oracles.** For many proximal operators known in closed-form, the Jacobians are trivial to find in closed-form. For example, the  $\ell_1$  norm has proximal operator given by soft-thresholding,  $\mathcal{T}_t$ . Since soft-thresholding occurs component-wise, this means that the Jacobian is a diagonal matrix, whose non-zero entries are 1 if  $b_i^{k+1/2}$  is above the threshold,  $-1$  if it is below the negative of the threshold, and 0 otherwise. In this case, it is possible to efficiently compute the vector-Jacobian oracle without forming the whole Jacobian to find

$$D\text{prox}_{t\|\cdot\|_1}(b^{k+1/2})^*u = \text{diag}(J_{T_t}(b^{k+1/2})) \circ u,$$

where  $a \circ b$  denotes Hadamard or component-wise multiplication. Here we handle the points of non-differentiability by using the value of the derivative at a point in a very small neighborhood of the non-differentiable point.

Other closed-form proximal operators have non-trivial Jacobians. For example, the proximal operator of the nuclear norm is given by

$$\mathbf{prox}_{t\|\cdot\|_*}(b^{k+1/2}) = U\mathcal{T}_t(\Sigma)V^*,$$

where  $b^{k+1/2} = U\Sigma V^*$  is the singular-value decomposition of  $b^{k+1/2}$  and  $\mathcal{T}_t$  is soft-thresholding on  $\Sigma$ . This has a non-trivial Jacobian because of the multi-valued nature of the SVD in the presence of repeated singular values. However, since all proximal operators are Lipschitz, we know that it is a.e.-differentiable. [13, Lemma IV.2] gives closed-form expressions for the Jacobian of this proximal operator that hold for simple and full-rank matrices. However, it is common that later iterations will involve low-rank matrices, which requires us to select an approximation of the vector-Jacobian products. We use the continuous extension of the closed-form vector-Jacobian product, which exists for all matrices which do not have any singular values exactly equal to  $t$ . We derive an expression for this extension in §C. For matrices with singular values exactly  $t$  we just evaluate at a point within the neighborhood of the matrix similar to how we handle the  $\ell_1$  norm.

Since  $D\hat{\mu}(y)^*v = \nabla_y \langle \hat{\mu}(y) \mid v \rangle$ , it is possible to apply well-known strategies to compute the gradient of a scalar-valued function. Most notably, reverse-mode automatic differentiation automates much of this section’s work [20]. For many proximal operators with closed-form expressions, reverse-mode automatic differentiation can differentiate the proximal operator without an analytic derivation of a closed-form for the vector-Jacobian oracle.

As an example we work out how to construct the oracle for  $r(b) = \|b\|_1 + \|b\|_2^2$  (a weighted sum of these norms is the regularizer in the elastic net [35]). The proximal operator can be evaluated by applying separability to find that it is given by a scaled form of soft-thresholding,

$$\mathbf{prox}_{tr(b)}(v) = \operatorname{argmin}_b \left( t\|b\|_1 + t\|b\|^2 + \frac{1}{2}\|b - v\|_2^2 \right) = \frac{1}{1 + 2t}\mathcal{T}_t(v).$$

By rewriting soft-thresholding as  $\mathcal{T}_t(v) = (v - t\mathbf{1})_+ - (-v - t\mathbf{1})_+$ , we can express this function in terms of elementary operations that are commonly supported by automatic differentiation libraries, meaning no work is required to construct the vector-Jacobian oracle.

## 2.3 Implementation

We have implemented the methods described above in SURE-CR, an open-source package available at

<https://github.com/cvxgrp/SURE-CR>.

It supports divergence computation via CVXPYlayers as well as via differentiation through FISTA and ADMM, and uses Hutch++ to estimate the divergence.

SURE-CR relies on an existing computational graph library, pyTorch [30], to enable GPU-acceleration in our solvers and to enable reverse-mode automatic differentiation. We have implemented a library to encode the linear operator  $\mathcal{A}$  as a computational flow graph. It is available at

[https://github.com/cvxgrp/torch\\_linops](https://github.com/cvxgrp/torch_linops).

This library adapts Barratt’s preconditioned conjugate gradient implementation [6] and implements randomized preconditioners including Nyström preconditioning [18].

By differentiating through FISTA and ADMM iterations, SURE-CR is able to scale to large problems. For example it can evaluate SURE for a matrix completion problem with  $b \in \mathbf{R}^{2000 \times 1000}$  and 10% of entries revealed, for which  $D\hat{\mu}(y)$  is a  $10^5 \times 10^5$  matrix (which of course is never formed) in 120 seconds on the server described in §3.

To apply SURE-CR to novel problems and regularizers, the user should adapt an example from §A by implementing their linear operator  $\mathcal{A}$  and  $\mathcal{A}^*$  as shown in §A.3 and implementing the proximal operator as a differentiable torch function. This can be done most easily by expressing it as the composition of built-in torch functions as shown in §A.2. In the event that a heuristic is used for the derivative of the proximal operator, it may be valuable to test that the heuristic and the true vector-Jacobian products found by CVXPYlayers agree.

SURE-CR currently uses at most one GPU; however, in hyperparameter sweep problems, users can run different experiments on different GPUs in parallel.

## 3 Numerical examples

In this section we report results of numerical examples of SURE-CR. We consider three problems, LASSO, matrix completion, and robust PCA, and for each one, problem instances ranging from small to large. For each instance we evaluate various estimates of SURE, as well as an estimate of the  $\ell_2$  risk obtained via a Monte Carlo method described below.

We carry out a few additional experiments that analyze the variance contributed by SURE itself in high-dimensions, and also, the variance contributed by our use of a randomized trace estimator. We will see that the latter is substantially smaller than the former.

Finally, in our last example, we show how SURE-CR can be used to carry out hyperparameter selection.

**Hyperparameter selection.** When selecting regularization parameters, we swept over the parameters—equally spaced on a logarithmic scale—on the largest problem size we planned to run. We then selected a value which had risk less than half the risk of the maximum likelihood estimator of  $\mu$  and had a high iteration count relative to the other runs in the sweep. We require the risk to be small in order to demonstrate SURE-CR in problem settings where the estimator is useful. The higher the iteration count, the longer SURE-CR takes to run since we have to differentiate through more iterations of the solver algorithm; accordingly, to give a better sense of worst-case runtime when using SURE-CR we prefer problem instances that gave higher iteration counts.

**SURE estimates.** In our first example, LASSO, we report the value of the analytical expression for SURE. In all examples we evaluate SURE using CVXPYlayers, where it was possible, *i.e.*, for the smaller problem instances. For each problem we use either ADMM or FISTA, depending on which was faster on small test problems.

**Monte Carlo  $\ell_2$  risk estimate.** Since we are using synthetic data and know  $\mu = \mathcal{A}\beta$ , we are able to use a Monte-Carlo method to approximate the risk as

$$R(\hat{\mu}) \approx \frac{1}{m} \sum_{i=1}^m \|\hat{\mu}(y_i) - \mu\|_2^2,$$

where  $y_i \stackrel{\text{i.i.d.}}{\sim} \mathcal{N}(\mu, \sigma^2 I)$ . (In practical problem settings, this Monte-Carlo estimation of  $\ell_2$  risk is not possible.)

**Computational platform.** We report timings for running SURE-CR on the Stanford University Institute for Computational and Mathematical Engineering’s DGX-1, with 8 Nvidia Tesla V100-SXM2-32GB-LS GPUs, an Intel Xeon E5-2698 v4 with 80 cores, 540GiB of memory, and 32GiB of GPU memory per GPU. (However, we were limited to only one GPU during our tests.)

**Overview of results.** The results are summarized in the tables below. Comparing the values of the various estimates of SURE and  $\ell_2$  risk across each row, we see that there is good agreement, except for the smallest problem instances. In §B, we show that recent works by Bellec and Zhang [9, 10] enables bounding the variance of SURE to be less than  $4\sigma^4 d + 2\sigma^2 R(\hat{\mu})$ . For our estimators, the risk scales about affinely with  $d$ , and therefore the standard deviation of SURE grows slower than its expectation, so we see asymptotic convergence to the true value in relative error.

For the largest instances of matrix completion and robust PCA, each of which have 2 million parameters, we are able to compute SURE in under two minutes. To our knowledge, there was no previously known method for computing SURE for such large instances.

### 3.1 LASSO

We compute SURE for LASSO problems, described in §1.3. We consider under-determined problems with  $p = 2d$ , for  $d = 250, 500, 2500, 5000, 25000$ .

**Data generation.** We draw the entries of the data matrix i.i.d. from a standard normal distribution. We pick  $\beta$  with  $d/20$  nonzero entries equal to a constant and use  $\sigma^2 = 2$ . We pick the value of the nonzero coefficients so that  $\frac{\|\mu\|_2^2}{\|\mu\|_2^2 + d\sigma^2} = 0.8$ . We sample one  $y$  independently from the rest of the data and select  $\lambda = 0.1\lambda_{\max}$  (defined in (3)).

For each instance we use SURE-CR with CVXPYlayers, SURE-CR with FISTA, the analytic SURE value computed against the solution CVXPYlayers found, and the Monte-Carlo estimate of the risk using CVXPY to solve the optimization problem. In its default configuration, CVXPYlayers has very low accuracy in moderate dimensions and does not raise warnings about the errors. To correct for this, we switched CVXPYlayer’s implicit linear system solver for its direct linear system solver; this did not significantly impact runtime on problems where it was giving accurate answer. We present both the risk and time values for each. When using CVXPYlayers, we report the value as \* when CVXPYlayers has a non-standard return status warning, raises an error, or takes more than 12 hours. The seed used to generate the Hutch++ queries and the sample point at which to compute SURE are the same for all problems of a given size. The results are given in Table 1.

**Table 1:** Values of coordinate-wise SURE estimates and computation times for five LASSO problem instances. Coordinate-wise SURE is given by  $\frac{\text{SURE}(\hat{\mu}, y)}{d}$  and is used to improve readability. Times given in seconds.

Dimensions		CVXPYlayers		FISTA		Analytic	MC risk
$d$	$p$	Value	Time	Value	Time		
250	500	0.51	252	0.51	2.54	0.52	0.48(<0.005)
500	1000	0.43	1929	0.37	2.89	0.40	0.50(<0.005)
2500	5000	*	*	0.58	3.10	0.57	0.51(<0.005)
5000	10000	*	*	0.47	9.19	0.46	0.53(<0.005)
25000	50000	*	*	0.58	287	0.58	0.54(<0.005)

**Table 2:** Values of coordinate-wise SURE estimates and computation times for five matrix completion problem instances. Coordinate-wise SURE is given by  $\frac{\text{SURE}(\hat{\mu}, y)}{d}$  and is used to improve readability. Times given in seconds.

Dimensions		CVXPYlayers		ADMM		MC risk
$d$	$p$	Value	Time	Value	Time	
20	200	1.15	1.51	1.16	5.20	1.33(0.01)
500	5000	0.86	2246	0.88	49.9	0.96(<0.005)
2000	$2 \times 10^4$	0.84	15866	0.84	45.1	0.90(<0.005)
$2 \times 10^4$	$2 \times 10^5$	*	*	1.69	41.2	1.70(<0.005)
$2 \times 10^5$	$2 \times 10^6$	*	*	0.74	114	0.74(<0.005)

## 3.2 Matrix completion

We compute SURE for matrix completion problems, described in §1.4. For all problems, we use  $d = 0.1mn$ ,  $\sigma^2 = 2$ , and  $\lambda = 0.25\lambda_{\max}$ . For the large problems used to generate Figure 1, we use  $m = 2000$ ,  $n = 1000$ ,  $d = 0.1mn = 200000$ . We use SURE-CR with CVXPYlayers and SURE-CR with ADMM to compute SURE in Table 2. We describe how we formed  $\mu$  and  $\beta$  below.

Since  $\mathcal{A}^*\mathcal{A} + \lambda I$  is a diagonal matrix, we replace the preconditioned conjugate gradient step of the ADMM updates with an exact inverse. This has no significant impact on the numerical accuracy of our algorithm, but does improve its runtime.

**Data generation.** We first generate  $\beta = U\Sigma V^* \in \mathbf{R}^{m \times n}$  with  $\max(5, 0.02n)$  non-zero singular values, which are uniformly distributed over  $[0, n]$ . The matrices  $U$  and  $V^*$  are generated by computing the SVD of a matrix where each entry is independent and identically distributed as uniform over  $[0, 1]$ . For the selection operator  $\mathcal{A}$ , we selected 10% of the entries at random without replacement. We then sampled  $y \sim \mathcal{N}(\mathcal{A}\beta, \sigma^2 I)$ .

**Quantifying Hutch++ uncertainty.** We verify that the uncertainty from using Hutch++ to estimate the divergence is dominated by the uncertainty inherent in SURE. For 20 sample points of  $y$ , we ran SURE-CR on each point 100 times. In Figure 1, we show in blue the distribution of the relative error between the SURE-CR values and the sample mean of the SURE-CR runs on that point: let  $\text{SURE-CR}(y, i)$  denote the random variable of the output of running SURE-CR on a point  $y$  with seed  $i$ . Then for samples  $y_1, y_2, \dots, y_{10\,020}$ , we plot the histogram of

$$\frac{\text{SURE-CR}(\hat{\mu}, y_i, 100i + j) - 100^{-1} \sum_{k=1}^{100} \text{SURE-CR}(\hat{\mu}, y_i, 100i + k)}{10\,000^{-1} \sum_{k=1}^{100} \sum_{\ell=21}^{10\,020} \text{SURE-CR}(\hat{\mu}, y_\ell, 100\ell + k)}$$

for  $i = 1, 2, \dots, 20$  and  $j = 1, 2, \dots, 100$ . We also plot the histogram of the relative error between 2000 evaluations of SURE-CR and the Monte-Carlo estimation of the risk. The uncertainty from the algorithm's randomization is small compared to SURE's uncertainty.

**SURE as estimate of risk.** The green histogram in Figure 1 shows that SURE-CR is within 2.5% of the Monte-Carlo risk at 2000 independent sample points. Precisely, the green histogram shows the histogram of the quantity

$$\frac{\text{SURE-CR}(\hat{\mu}, y_i, i) - 10\,000^{-1} \sum_{j=2001}^{12\,000} \|\hat{\mu}(y_j) - \mu\|_2^2}{10\,000^{-1} \sum_{j=2001}^{12\,000} \|\hat{\mu}(y_j) - \mu\|_2^2}$$

for  $i = 1, 2, \dots, 2000$  and independent samples  $y_1, y_2, \dots, y_{12\,000}$ . This shows SURE is a good estimate of the true risk.

**Non-differentiability.** In around 5% of the 2000 samples used to generate the green histogram in Figure 1, we observed that our approximation of  $\hat{\mu}$  was non-differentiable. However, those samples are indistinguishable from the other samples in the histogram, showing that our heuristic is effective at approximating the vector-Jacobian products for  $\hat{\mu}$  and still provide a good estimate of risk.

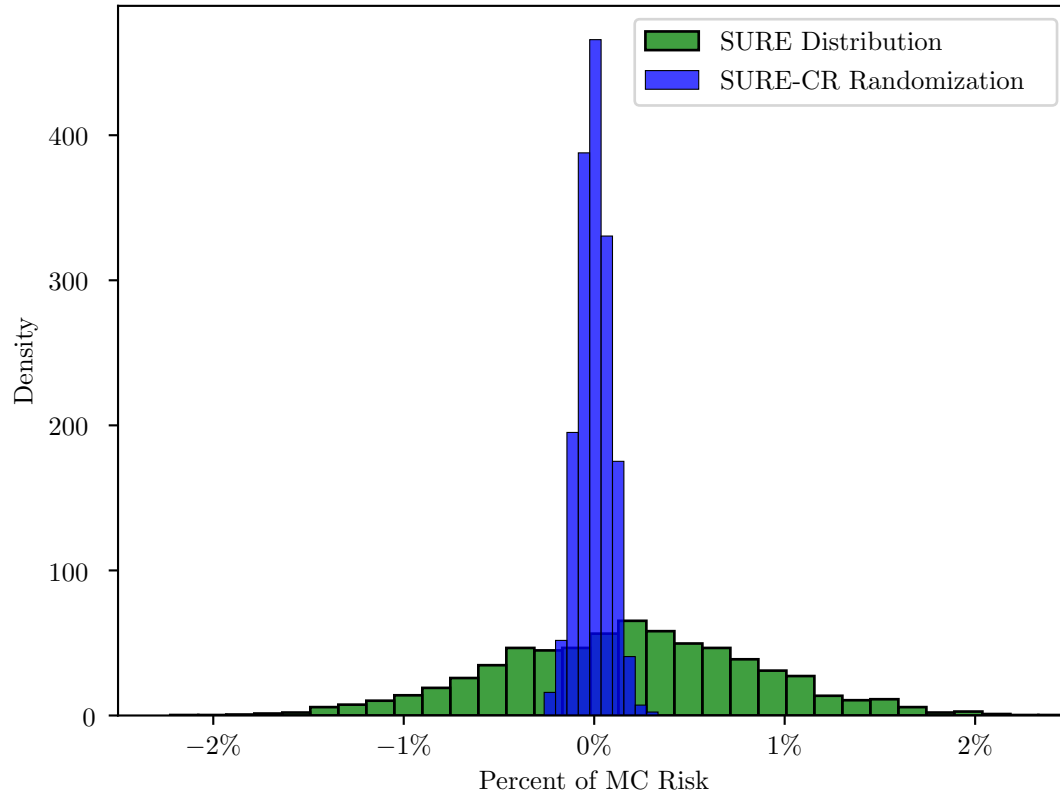


**Figure 1:** The green histogram is the relative error between SURE at various sample points against the Monte-Carlo risk. The blue histogram shows the relative error between SURE-CR at a sample point and the mean of 100 runs of SURE-CR at that point.

**Table 3:** Values of coordinate-wise SURE estimates and computation times for five robust PCA problem instances. Coordinate-wise SURE is given by  $\frac{\text{SURE}(\hat{\mu}, y)}{d}$  and is used to improve readability. Times given in seconds.

Dimensions		CVXPYlayers		ADMM		MC risk
$d$	$p$	Value	Time	Value	Time	
100	200	5.14	1.15	5.13	16.0	5.01(0.006)
2500	5000	0.53	115	0.53	19.9	0.59(<0.005)
10000	$2 \times 10^4$	0.31	1116	0.31	21.5	0.34(<0.005)
$2.5 \times 10^5$	$5 \times 10^5$	*	*	0.27	22.1	0.27(<0.005)
$1 \times 10^6$	$2 \times 10^6$	*	*	0.44	31.4	0.44(<0.005)

### 3.3 Robust PCA

We also tested SURE on robust PCA problems, described in §1.4. For all problems, we use  $m = n$ ,  $\sigma^2 = 2$ ,  $\lambda = 0.16\lambda_{\max}$ , and  $\gamma = 0.057\gamma_{\max}$ . For the large problems used to generate Figure 2, we used  $m = n = 1000$ . We use SURE-CR with CVXPYlayers and SURE-CR with ADMM to compute SURE in Table 3.

**Data generation.** We select  $S$  with  $\max(10, 10^{-4}n^2)$  non-zero entries drawn from a uniform distribution over  $[0, 100]$ . We select  $L$  with rank  $\max(5, 0.02n)$  and singular values distributed uniformly over  $[0, n]$ . We sampled  $y \sim \mathcal{N}(L + S, \sigma^2 I)$ .

**SURE as estimate of risk.** Figure 2 shows the histogram of the relative error compared to the Monte-Carlo estimate of the risk for  $m = n = 1000$  and the histogram of the variance from the randomization in SURE-CR for  $m = n = 1000$ . We ran SURE-CR on 2000 sample points and use 10 000 samples for the Monte-Carlo estimate. We observed only one sample for which SURE-CR diverged from the Monte-Carlo risk by more than 3%.

### 3.4 SURE for hyperparameter selection

In this experiment, we aim to select an optimal hyperparameter for matrix completion. We use the same setup as in §3.2 with  $m = 2000$  and  $n = 1000$ , except we now draw a single sample  $y$ .

We then ran a grid search over  $\lambda$ , varying it exponentially over  $[1, 2\lambda_{\max}]$ , where  $\lambda_{\max}$  is the smallest  $\lambda$  for which  $\hat{\beta}(y) = 0$ . We drew a single sample of  $y$ , and then for

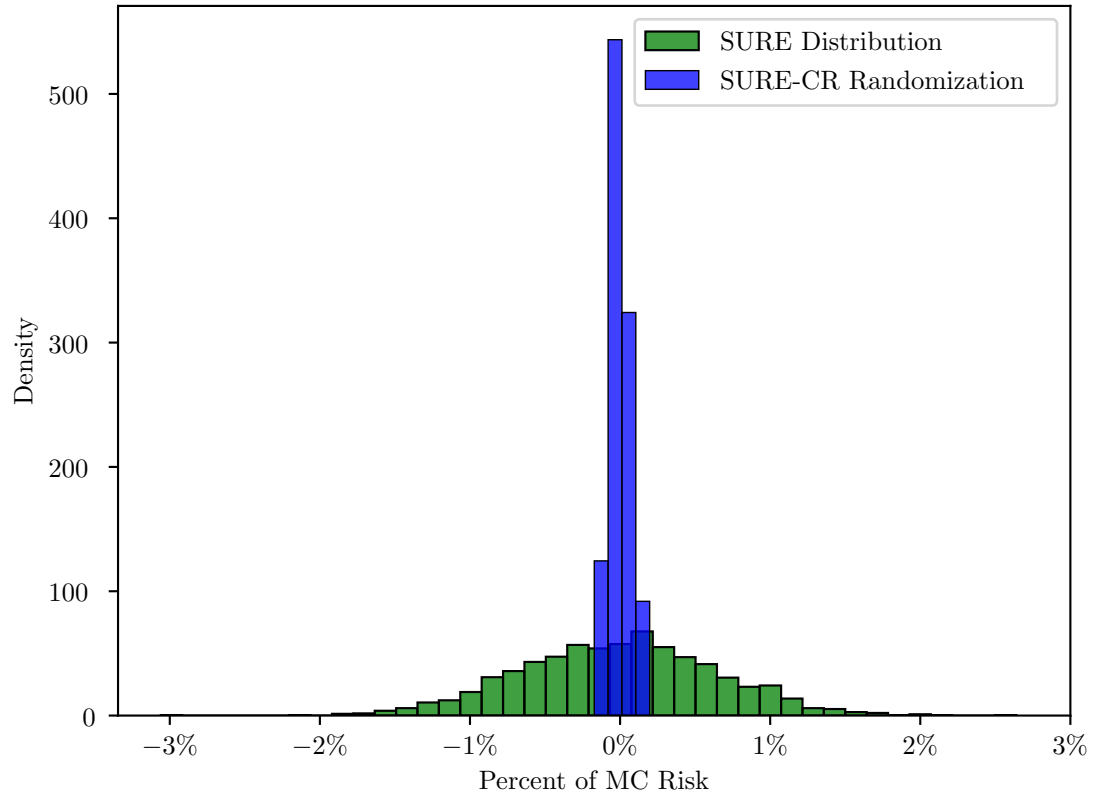


**Figure 2:** The histogram of the relative error between SURE-CR run at different sample points and the Monte-Carlo risk.

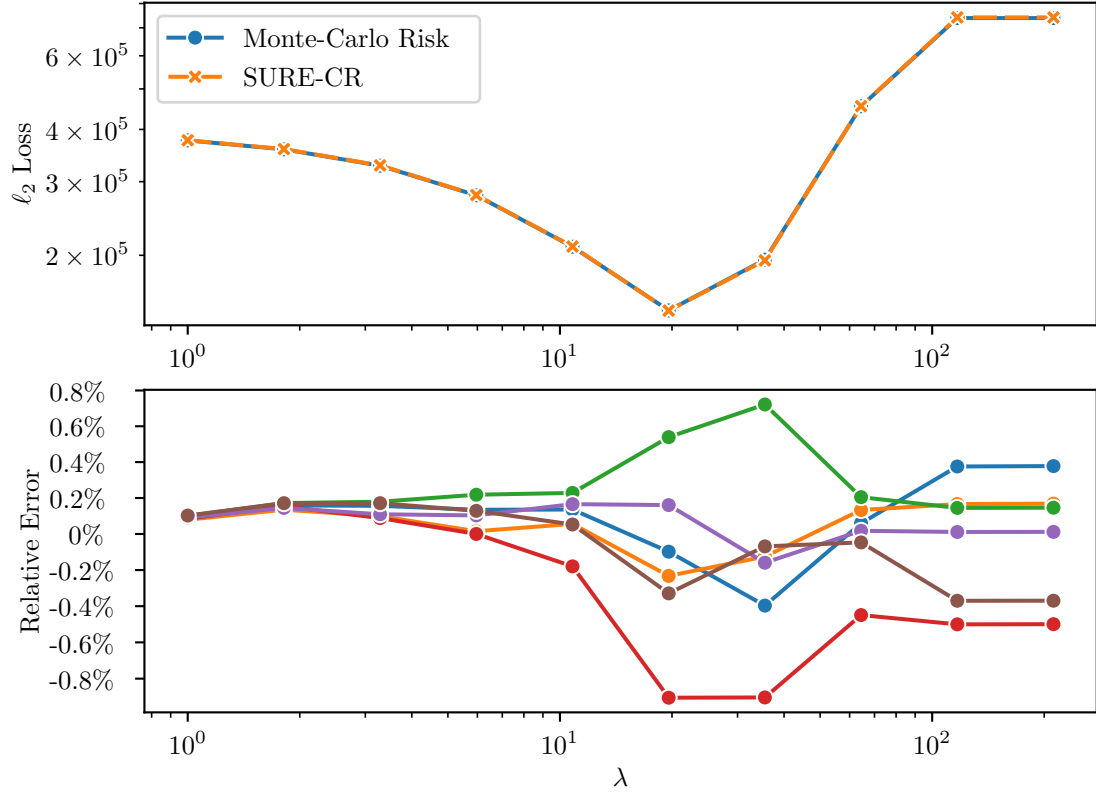


**Figure 3:** *Top.* SURE-CR and Monte-Carlo estimate of  $\ell_2$  risk as a function of the hyperparameter. A single sample of  $y$  was used for all of the SURE-CR runs. The two lines are visually indistinguishable. *Bottom.* Relative error plots for the SURE-CR sweep run on 6 independent samples of  $y$ . The Monte Carlo estimate and the computed SURE value differ by less than 1%.

each  $\lambda$  we ran SURE-CR with ADMM. We then computed a Monte-Carlo estimation of the risk for each  $\lambda$ . Figure 3, shows that the risk versus  $\lambda$  curves are functionally indistinguishable. We also show that for 6 independent samples of  $y$ , the relative error was consistently below 0.9%.

## Acknowledgments

We thank Mert Pilanci for many helpful comments during a talk about this project. We also thank Raphael Meyer for help with Hutch++.

Parth Nobel was supported in part by the National Science Foundation Graduate Research Fellowship Program under Grant No. DGE-1656518. Any opinions, findings, and conclusions or recommendations expressed in this material are those of the author(s) and do not necessarily reflect the views of the National Science Foundation.

Stephen Boyd was partially supported by ACCESS (AI Chip Center for Emerging Smart Systems), sponsored by InnoHK funding, Hong Kong SAR, and by Office of Naval Research grant N00014-22-1-2121. Emmanuel Candès was supported by the Office of Naval Research grant N00014-20-1-2157, the National Science Foundation grant DMS-2032014, the Simons Foundation under award 814641, and the ARO grant 2003514594.

## References

- [1] M. Abadi, A. Agarwal, P. Barham, E. Brevdo, Z. Chen, C. Citro, G. S. Corrado, A. Davis, J. Dean, M. Devin, S. Ghemawat, I. Goodfellow, A. Harp, G. Irving, M. Isard, Y. Jia, R. Jozefowicz, L. Kaiser, M. Kudlur, J. Levenberg, D. Mané, R. Monga, S. Moore, D. Murray, C. Olah, M. Schuster, J. Shlens, B. Steiner, I. Sutskever, K. Talwar, P. Tucker, V. Vanhoucke, V. Vasudevan, F. Viégas, O. Vinyals, P. Warden, M. Wattenberg, M. Wicke, Y. Yu, and X. Zheng. TensorFlow: Large-scale machine learning on heterogeneous systems, 2015. Software available from tensorflow.org.
- [2] A. Agrawal, B. Amos, S. Barratt, S. Boyd, S. Diamond, and Z. Kolter. Differentiable convex optimization layers. In *Advances in Neural Information Processing Systems*, 2019.
- [3] A. Agrawal, S. Barratt, S. Boyd, E. Busseti, and W. Moursi. Differentiating through a cone program. *Journal of Applied and Numerical Optimization*, 1(2):107–115, 2019.

- [4] A. Agrawal, A. N. Modi, A. Passos, A. Lavoie, A. Agarwal, A. Shankar, I. Ganichev, J. Levenberg, M. Hong, R. Monga, and S. Cai. TensorFlow Eager: A multi-stage, Python-embedded DSL for machine learning. In *Proceedings of the 2nd SysML Conference*, 2019.
- [5] B. Amos and J. Z. Kolter. OptNet: Differentiable optimization as a layer in neural networks. In *Proceedings of the 34th International Conference on Machine Learning*, volume 70 of *Proceedings of Machine Learning Research*, pages 136–145. PMLR, 2017.
- [6] S. Barratt. torch\_cg. [https://github.com/sbarratt/torch\\_cg](https://github.com/sbarratt/torch_cg), Mar. 2019.
- [7] A. Beck. *First-order methods in optimization*. SIAM, 2017.
- [8] A. Beck and M. Teboulle. A fast iterative shrinkage-thresholding algorithm for linear inverse problems. *SIAM Journal on Imaging Sciences*, 2(1):183–202, 2009.
- [9] P. C. Bellec and C.-H. Zhang. De-biasing convex regularized estimators and interval estimation in linear models, 2021. arXiv:1912.11943v4 [math.ST].
- [10] P. C. Bellec and C.-H. Zhang. Second-order Stein: SURE for SURE and other applications in high-dimensional inference. *The Annals of Statistics*, 49(4):1864–1903, 2021.
- [11] Y. Bengio, N. Léonard, and A. Courville. Estimating or propagating gradients through stochastic neurons for conditional computation, 2013. arXiv:1308.3432 [cs.LG].
- [12] S. Boyd, N. Parikh, and E. Chu. *Distributed optimization and statistical learning via the alternating direction method of multipliers*. Now Publishers Inc, 2011.
- [13] E. J. Candès, C. A. Sing-Long, and J. D. Trzasko. Unbiased risk estimates for singular value thresholding and spectral estimators. *IEEE Transactions on Signal Processing*, 61(19):4643–4657, 2013.
- [14] A. Chambolle and T. Pock. A first-order primal-dual algorithm for convex problems with applications to imaging. *Journal of Mathematical Imaging and Vision*, 40(1):120–145, 2011.
- [15] G. Chierchia, E. Chouzenoux, P. L. Combettes, and J.-C. Pesquet. The proximity operator repository. <http://proximity-operator.net/>, 2016.

- [16] S. Diamond, V. Sitzmann, F. Heide, and G. Wetzstein. Unrolled optimization with deep priors, 2018. arXiv:1705.08041 [cs.CV].
- [17] L. Evans and R. Gariepy. *Measure Theory and Fine Properties of Functions, Revised Edition*. CRC Press, 2015.
- [18] Z. Frangella, J. A. Tropp, and M. Udell. Randomized Nystrom preconditioning, 2021. arXiv:2110.02820 [math.NA].
- [19] X. Glorot, A. Bordes, and Y. Bengio. Deep sparse rectifier neural networks. In G. Gordon, D. Dunson, and M. Dudík, editors, *Proceedings of the Fourteenth International Conference on Artificial Intelligence and Statistics*, volume 15 of *Proceedings of Machine Learning Research*, pages 315–323, Fort Lauderdale, FL, USA, 11–13 Apr 2011. PMLR.
- [20] A. Griewank. On automatic differentiation. *Mathematical Programming: Recent Developments and Applications*, 6(6):83–107, 1989.
- [21] A. Griewank and A. Walther. *Evaluating derivatives: principles and techniques of algorithmic differentiation*. SIAM, 2008.
- [22] M. R. Hestenes and E. Stiefel. Methods of conjugate gradients for solving linear systems. *Journal of Research of the National Bureau of Standards*, 49(6):409, 1952.
- [23] M. F. Hutchinson. A stochastic estimator of the trace of the influence matrix for Laplacian smoothing splines. *Communications in Statistics — Simulation and Computation*, 18(3):1059–1076, 1989.
- [24] A. Krylov. On the numerical solution of equation by which are determined in technical problems the frequencies of small vibrations of material systems. *Izvestiya Akademii Nauk SSSR*, 7:491–539, 1931.
- [25] R. A. Meyer, C. Musco, C. Musco, and D. Woodruff. Hutch++: Optimal stochastic trace estimation. *Proceedings of the 4th Symposium on Simplicity in Algorithms (SOSA)*, 2021.
- [26] J. J. Moreau. Fonctions convexes duales et points proximaux dans un espace Hilbertien. *Comptes Rendus de l’Académie des Sciences de Paris*, 255(22):2897–2899, 1962.

- [27] Y. Nesterov. Gradient methods for minimizing composite functions. *Mathematical Programming*, 140:125–161, 2013.
- [28] J. Nocedal and S. Wright. *Numerical Optimization*. Springer, 2006.
- [29] N. Parikh and S. Boyd. Proximal algorithms. *Foundations and Trends in Optimization*, 1(3):127–239, 2014.
- [30] A. Paszke, S. Gross, F. Massa, A. Lerer, J. Bradbury, G. Chanan, T. Killeen, Z. Lin, N. Gimelshein, L. Antiga, A. Desmaison, A. Kopf, E. Yang, Z. DeVito, M. Raison, A. Tejani, S. Chilamkurthy, B. Steiner, L. Fang, J. Bai, and S. Chintala. PyTorch: An imperative style, high-performance deep learning library. In *Advances in Neural Information Processing Systems*, pages 8024–8035, 2019.
- [31] J. R. Shewchuk. An introduction to the conjugate gradient method without the agonizing pain. <https://dl.acm.org/doi/book/10.5555/865018>, 1994.
- [32] N. Simon, J. Friedman, and T. Hastie. A blockwise descent algorithm for group-penalized multiresponse and multinomial regression, 2013. arXiv:1311.6529 [stat.CO].
- [33] C. M. Stein. Estimation of the mean of a multivariate normal distribution. *The Annals of Statistics*, 9(6):1135–1151, 1981.
- [34] S. Wang, S. Fidler, and R. Urtasun. Proximal deep structured models. In D. Lee, M. Sugiyama, U. Luxburg, I. Guyon, and R. Garnett, editors, *Advances in Neural Information Processing Systems*, volume 29. Curran Associates, Inc., 2016.
- [35] H. Zou and T. Hastie. Regularization and variable selection via the elastic net. *Journal of the Royal Statistical Society: Series B (Statistical Methodology)*, 67(2):301–320, 2005.
- [36] H. Zou, T. Hastie, and R. Tibshirani. On the “degrees of freedom” of the LASSO. *The Annals of Statistics*, 35(5):2173–2192, 2007.

## A Code examples

### A.1 CVXPYlayers — LASSO

```
import cvxpy as cp

import surecr

X, y, variance, lambda_val = ... # Generate data

beta_cvx = cp.Variable(X.shape[1])
y_cvx = cp.Parameter(y.shape[0])
prob = cp.Problem(
    cp.Minimize(
        1/ 2 * cp.sum_squares(X @ beta_cvx - y_cvx)
        + lambda_val * cp.pnorm(beta_cvx, 1)
    )
)
solver = surecr.CVXPYSolver(prob, y_cvx, [beta_cvx], lambda b: X @ b)
sure = surecr.SURE(variance, solver)
cvx_sure_val = sure.compute(y)
```

### A.2 LASSO

```
import torch
import surecr
import linops as lo

X, y, variance, lambda_val = ... # Generate data

d, p = X.shape
A = lo.aslinearoperator(X.cuda())
y_cuda = y.cuda()
def prox(v, t):
    return torch.relu(v - lambda_val * t) - torch.relu(-v -
        lambda_val * t)
```

```

solver = surecr.FISTASolver(
    A, prox, torch.zeros(p).cuda(),
    device=y_cuda.device)
sure = surecr.SURE(variance, solver)

sure_val = sure.compute(y_cuda)

```

### A.3 Matrix completion

```

import torch
import surecr
import surecr.prox_lib as pl
import linops as lo

revealed_indices, y, variance, lambda_val, m, n = ... # Generate data

class SelectionOperator(lo.LinearOperator):
    def __init__(self, shape, idxs):
        self._shape = shape
        self._adjoint = _AdjointSelectionOperator(idxs,
            (self._shape[1], self._shape[0]), self)
        self._idxs = idxs

    def _matmul_impl(self, X):
        return X[self._idxs]

    def solve_I_p_lambda_AT_A_x_eq_b(self, lambda_, b):
        LHS = torch.ones_like(b)
        LHS[self._idxs] += lambda_
        return b / LHS

class _AdjointSelectionOperator(lo.LinearOperator):
    def __init__(self, idxs, shape, adjoint):
        self._shape = shape
        self._adjoint = adjoint

```

```

        self._idxs = idxs

    def _matmul_impl(self, y):
        z = torch.zeros(self.shape[0], dtype=y.dtype, device=y.device)
        z[self._idxs] = y
        return z.reshape(-1)

d = len(revealed_indices)
p = m * n
A = SelectionOperator((d, p), revealed_indices)
y_cuda = y.cuda()

# Generates a function that applies singular value thresholding,
# which uses a
# continuous extension of the derivative for the .backward method.
prox = pl.make_scaled_prox_nuc_norm((m, n), lambda_val)

solver = surecr.ADMMSolver(A, prox, torch.zeros(p).cuda(), device=
    y_cuda.device)
sure = surecr.SURE(variance, solver)

sure_val = sure.compute(y_cuda)

```

## A.4 Robust PCA

```

import torch
import surecr
import surecr.prox_lib as pl
import linops as lo

y, variance, lambda_val, gamma_val, m, n = ... # Generate data

d = m * n
p = 2 * d
A = lo.hstack([lo.IdentityOperator(d), lo.IdentityOperator(d)])

```

```

y_cuda = y.cuda()

# Generates a function that applies singular value thresholding,
# which uses a
# continuous extension of the derivative for the .backward method.
prox_L = pl.make_scaled_prox_nuc_norm((m, n), lambda_val)

def prox_S(v, t):
    return torch.relu(v - gamma_val * t) - torch.relu(-v - gamma_val
    * t)

def prox(v, t):
    return torch.hstack([
        prox_L(v[:d], t), prox_S(v[d:], t)
    ])

solver = surecr.ADMMSolver(A, prox, torch.zeros(p).cuda(), device=
    y_cuda.device)
sure = surecr.SURE(variance, solver)

sure_val = sure.compute(y_cuda)

```

## B Bound on the variance of SURE

In [10, Theorem 3.2], it is shown that for convexly regularized least squares

$$\text{var}(\text{SURE}(\hat{\mu}, y)) \leq \mathbf{E}[(\text{SURE}(\hat{\mu}, y) - \|\hat{\mu}(y) - \mu\|_2^2)^2] + \sigma^4 d$$

and

$$(\text{SURE}(\hat{\mu}, y) - \|\hat{\mu}(y) - \mu\|_2^2)^2 \leq 2\sigma^2(\|y - \hat{\mu}(y)\|_2^2 + \text{SURE}(\hat{\mu}, y))$$

almost surely. By applying algebraic manipulation and SURE's unbiasedness, we can find that

$$\text{var}(\text{SURE}(\hat{\mu}, y)) \leq 3\sigma^4 d - 4\sigma^4 \mathbf{E}[\nabla \cdot \hat{\mu}(y)] + 4\sigma^2 R(\hat{\mu}).$$

In [9, Proposition 5.3], it is shown that  $D\hat{\mu}(y)$  is almost surely positive semi-definite and that  $\|D\hat{\mu}(y)\|_{\text{Op}} \leq 1$  almost surely. This suggests that  $\nabla \cdot \hat{\mu}(y) =$

$\text{Tr}(D\hat{\mu}(y)) \in [0, d]$  almost surely and lets us conclude that

$$\text{var}(\text{SURE}(\hat{\mu}, y)) \leq 3\sigma^4 d + 4\sigma^2 R(\hat{\mu}).$$

## C Differentiating the proximal operator of the nuclear norm

The proximal operator of the nuclear norm is given by a spectral function  $F(X)$  such that  $F(X) = UF(\Sigma)V^T$  where  $U, \Sigma, V^T$  are the full SVD of  $X$  and where  $F(\Sigma)$  applies the function  $\mathcal{T}_t(\sigma) = (\sigma - t)_+$  elementwise to all entries of  $\Sigma$ .

We assume that  $X, Z, \Sigma, \zeta, \Gamma, \Delta \in \mathbf{R}^{m \times n}$ ,  $U \in \mathbf{R}^{m \times m}$ ,  $V \in \mathbf{R}^{n \times n}$ , and that  $\Omega_U, \Omega_V, \Omega_\Sigma$  are linear operators from  $\mathbf{R}^{m \times n}$  to  $\mathbf{R}^{m \times n}$ . Without loss of generality, we assume  $m \geq n$ . A simple matrix is one without repeated singular values.

### C.1 Gradient for full-rank and simple matrices

[13] gives that for simple and full-rank  $X$ :

$$(DF(X)) \Delta = U ((\Omega_U \Delta) F(\Sigma) + (\Omega_\Sigma \Delta) + F(\Sigma)(\Omega_V \Delta)) V^T$$

where

$$(\Omega_U \Delta)_{ij} = \begin{cases} 0 & \text{if } i = j \\ -\frac{1}{\sigma_i^2 - \sigma_j^2} (\sigma_j (U^T \Delta V)_{ij} + \sigma_i (U^T \Delta V)_{ji}) & \text{if } i \neq j \wedge i \leq n, \\ \frac{1}{\sigma_j} (U^T \Delta V)_{ij} & \text{else} \end{cases}$$

$$(\Omega_V \Delta)_{ij} = \begin{cases} 0 & \text{if } i = j \\ \frac{1}{\sigma_i^2 - \sigma_j^2} (\sigma_i (U^T \Delta V)_{ij} + \sigma_j (U^T \Delta V)_{ji}) & \text{else} \end{cases},$$

and

$$(\Omega_\Sigma \Delta)_{ij} = \begin{cases} \mathcal{T}'_t(\sigma_i) (U^T \Delta V)_{ii} & \text{if } i = j \\ 0 & \text{if } i \neq j \end{cases}.$$

In order to find the adjoint of this mapping we begin by constructing a convenient orthonormal basis of  $\mathbf{R}^{m \times n}$ . We then project the desired quantity  $(DF(X))^* Z$  onto the basis vectors. We can then weight and sum the basis elements to form  $(DF(X))^* Z$ .

Let  $\{E^{ij}\}_{i,j \in [m] \times [n]}$  be the standard basis of  $\mathbf{R}^{m \times n}$ , *i.e.*,  $E_{k\ell}^{ij} = 1$  iff  $i = k$  and  $j = \ell$  and is otherwise 0. Let  $\Delta^{ij} = u_i v_j^T$ . Critically,  $U^T \Delta^{ij} V = E^{ij}$  which will greatly simplify the mappings given above. For notational simplicity, let  $\zeta = U^T Z V$ .

Evaluating the projection yields

$$\langle (DF(X))^* Z \mid \Delta^{ij} \rangle = \begin{cases} \mathcal{T}'_t(\sigma_i) \zeta_{ii} & \text{if } i = j \\ \frac{\mathcal{T}_t(\sigma_j)}{\sigma_j} \zeta_{ij} & \text{if } i > n \\ \frac{\sigma_j \mathcal{T}_t(\sigma_i) - \sigma_i \mathcal{T}_t(\sigma_j)}{\sigma_i^2 - \sigma_j^2} \zeta_{ij} + \frac{\sigma_j \mathcal{T}_t(\sigma_i) - \sigma_i \mathcal{T}_t(\sigma_j)}{\sigma_i^2 - \sigma_j^2} \zeta_{ji} & \text{else} \end{cases}$$

This projection is not defined for some basis elements whenever there exists  $i \neq j$  such that  $\sigma_i = \sigma_j$  or  $i$  such that  $\sigma_i = 0$ .

## C.2 Extension by continuity to all matrices

Following [13], we seek to extend the projection of  $(DF(X))^* Z$  by continuity to the situation where there exists  $i \neq j$ , such that  $\sigma_i = \sigma_j =: \sigma$  or there exists  $\sigma_i = 0$ . Note that the projection is only ill-defined for basis elements  $\Delta^{ij}$  such that  $i \leq n$  and  $i \neq j$ . Since simple and full-rank matrices are dense in  $\mathbf{R}^{m \times n}$ , we will consider a sequence of matrices  $X^{(k)}$  such that each  $X^{(k)}$  is simple and full-rank and  $\lim_{k \rightarrow \infty} X^{(k)} = X$ .

From [13], we have that for  $i \neq j$  such that  $\sigma_i = \sigma_j =: \sigma > 0$ ,

$$\frac{\sigma_i^{(k)} \mathcal{T}_t(\sigma_i^{(k)}) - \sigma_j^{(k)} \mathcal{T}_t(\sigma_j^{(k)})}{\left(\sigma_i^{(k)}\right)^2 - \left(\sigma_j^{(k)}\right)^2} \zeta_{ij} \rightarrow \left(\frac{1}{2} \mathcal{T}'_t(\sigma) + \frac{1}{2} \frac{\mathcal{T}_t(\sigma)}{\sigma}\right) \zeta_{ij},$$

and that for  $i \neq j$  such that  $\sigma_i = \sigma_j = 0$ ,

$$\frac{\sigma_i^{(k)} \mathcal{T}_t(\sigma_i^{(k)}) - \sigma_j^{(k)} \mathcal{T}_t(\sigma_j^{(k)})}{\left(\sigma_i^{(k)}\right)^2 - \left(\sigma_j^{(k)}\right)^2} \zeta_{ij} \rightarrow \mathcal{T}'_t(\sigma) \zeta_{ij}.$$

A symmetric version of the argument from [13] gives that for  $i \neq j$  such that  $\sigma_i = \sigma_j =: \sigma > 0$ ,

$$\frac{\sigma_j^{(k)} \mathcal{T}_t(\sigma_i^{(k)}) - \sigma_i^{(k)} \mathcal{T}_t(\sigma_j^{(k)})}{\left(\sigma_i^{(k)}\right)^2 - \left(\sigma_j^{(k)}\right)^2} \zeta_{ji} \rightarrow \left(\frac{1}{2} \mathcal{T}'_t(\sigma) - \frac{1}{2} \frac{\mathcal{T}_t(\sigma)}{\sigma}\right) \zeta_{ji},$$

and for  $i \neq j$  such that  $\sigma_i = \sigma_j = 0$ ,

$$\frac{\sigma_j^{(k)} \mathcal{T}_t(\sigma_i^{(k)}) - \sigma_i^{(k)} \mathcal{T}_t(\sigma_j^{(k)})}{\left(\sigma_i^{(k)}\right)^2 - \left(\sigma_j^{(k)}\right)^2} \zeta_{ji} \rightarrow 0.$$

Lastly, note that when  $\sigma_j = 0$ ,

$$\lim_{\sigma_j^{(k)} \rightarrow 0} \frac{\mathcal{T}_t(\sigma_j^{(k)})}{\sigma_j^{(k)}} = \mathcal{T}'_t(0).$$

In summary, the continuous extension of  $\langle (DF(X))^* Z, \Delta^{ij} \rangle$  for all  $X$  is given by

$$\Gamma_{ij} = \begin{cases} \mathcal{T}'_t(\sigma_i) \zeta_{ii} & \text{if } i = j \\ R(\sigma_j) \zeta_{ij} & \text{if } i > n \\ Q(\sigma_i, \sigma_j) \zeta_{ij} + T(\sigma_i, \sigma_j) \zeta_{ji} & \text{else} \end{cases}$$

where

$$R(\sigma) = \begin{cases} \frac{\mathcal{T}_t(\sigma)}{\sigma} & \text{if } \sigma > 0 \\ \mathcal{T}'_t(\sigma) & \text{if } \sigma = 0 \end{cases},$$

$$Q(\sigma_i, \sigma_j) = \begin{cases} \frac{1}{2} \mathcal{T}'_t(\sigma) + \frac{1}{2} \frac{\mathcal{T}_t(\sigma)}{\sigma} & \text{if } \sigma_i = \sigma_j =: \sigma > 0 \\ \mathcal{T}'_t(0) & \text{if } \sigma_i = \sigma_j = 0 \\ \frac{\sigma_i \mathcal{T}_t(\sigma_i) - \sigma_j \mathcal{T}_t(\sigma_j)}{\sigma_i^2 - \sigma_j^2} & \text{else} \end{cases},$$

and

$$T(\sigma_i, \sigma_j) = \begin{cases} \frac{1}{2} \mathcal{T}'_t(\sigma) - \frac{1}{2} \frac{\mathcal{T}_t(\sigma)}{\sigma} & \text{if } \sigma_i = \sigma_j =: \sigma > 0 \\ 0 & \text{if } \sigma_i = \sigma_j = 0 \\ \frac{\sigma_j \mathcal{T}_t(\sigma_i) - \sigma_i \mathcal{T}_t(\sigma_j)}{\sigma_i^2 - \sigma_j^2} & \text{else} \end{cases}.$$

### C.3 Numerically stable computation

Constructing  $\Delta^{ij}$  in order to evaluate  $\sum_{i=1}^m \sum_{j=1}^n \Gamma_{ij} \Delta^{ij}$  is numerically unstable in high dimensions.

However, some simple algebra gives that

$$\begin{aligned} \sum_{i=1}^m \sum_{j=1}^n \Gamma_{ij} \Delta^{ij} &= U U^T \left( \sum_{i=1}^m \sum_{j=1}^n \Gamma_{ij} \Delta^{ij} \right) V V^T = U \left( \sum_{i=1}^m \sum_{j=1}^n \Gamma_{ij} U^T \Delta^{ij} V \right) V^T \\ &= U \left( \sum_{i=1}^m \sum_{j=1}^n \Gamma_{ij} E^{ij} \right) V^T = U \Gamma V^T. \end{aligned}$$

Experimentally, evaluating  $U \Gamma V^T$  is numerically stable.